IEEE Access
Multidisciplinary | Rapid Review | Open Access Journal

Received June 9, 2020, accepted July 2, 2020, date of publication July 6, 2020, date of current version July 17, 2020.

Digital Object Identifier 10.1109/ACCESS.2020.3007516

A New Algorithm for Displacement Measurement Using Self-Mixing Interferometry With Modulated Injection Current

HAN WANG, YUXI RUAN, (Associate Member, IEEE), YANGUANG YU, (Senior Member, IEEE), QINGHUA GUO, (Senior Member, IEEE), JIANGTAO XI, (Senior Member, IEEE), AND JUN TONG, (Member, IEEE)

School of Electrical, Computer and Telecommunications Engineering, University of Wollongong, Northfields Avenue, Wollongong, NSW 2522, Australia

Corresponding author: Yanguang Yu (yanguang@uow.edu.au)

ABSTRACT Using self-mixing interferometry (SMI) with a periodical modulated injection current, high resolution displacement sensing can be achieved by retrieving the initial phase of an SMI signal at each modulation period. However, the existing initial-phase-based detection methods can only obtain a single point measurement of displacement within each single modulation period. Thus, they are only effective when the target is subject to slow movement, or the injection current is modulated by a signal of very high frequency, which are not practical in many applications. In this work, a new method is proposed to tackle the problem. Firstly, a reference signal is obtained by setting the target still. Then Fast Fourier Transform and its inverse (FFT/IFFT) are applied to the reference signal and the SMI signal, leading to a formulation to obtain the SMI signal phase, which enables the SMI system to retrieve the time varying displacement in each modulation period. As the proposed method is able to measure displacement at multiple discrete time instances (dependent on the number of samples for FFT), the measurement resolution is significantly improved over existing method. Hence, the measurement capability of the SMI system is enhanced greatly. Both simulation and experiments are conducted and the results are presented to verify the proposed algorithm.

INDEX TERMS Displacement measurement, semiconductor lasers, laser diode, self-mixing interferometry, fast Fourier transform, time-frequency analysis.

I. INTRODUCTION

When a fraction of external optical feedback re-enters the cavity of a laser diode (LD), the laser intensity and optical frequency will alter. Such a laser diode system is often called as self-mixing interferometry (SMI), the modulated laser intensity is called an SMI signal. As a promising noncontact sensing technology, SMI has attracted much attention of researchers in recent decades due to its low cost in implementation, and ease in optical alignment. Various SMI-based sensing applications have been reported, including the measurement of displacement, velocity, vibration, laser related parameters, thickness, mechanical resonance [1]–[7], etc. Recently, SMI-based sensing has been extended for imaging, material parameter measurement, near-field microscopy, chaotic radar, acoustic detection, biomedical applications [8]–[12], etc.

Displacement measurement is one of the important applications of SMI-based sensing. A typical SMI-based displacement measurement system contains just an LD, a lens and a target to be measured. In a class of SMI-based displacement measurements, the LD is set with a constant bias injection current. For example, in 1995, Donati, *et al.* firstly developed a fringe counting method based on the fact that each fringe on an SMI waveform corresponds to a half-wavelength ($\lambda/2$) displacement of a moving target [13]. This sensing system can measure displacement with a maximum dynamic range of 1.2 m. The work in [13] was further improved to enhance measurement resolution by Merlo and Donati in 1997 [14]. The work in [14] implemented a phase unwrapping algorithm to reconstruct displacement from an SMI signal and achieved the measurement with the order

The associate editor coordinating the review of this manuscript and approving it for publication was Chao Zuo.

of $\lambda/13.5$. However, the reconstruction algorithm can only work for a weak feedback level where each fringe of an SMI signal has approximately a sinusoidal shape. When an LD receives moderated optical feedback, the fringes will change to saw-tooth-like shape. In 1998, Servagent, *et al.* proposed to perform linear interpolation within each fringe to obtain displacement by using the saw-tooth feature of such SMI signals [15]. The results showed that the proposed method can achieve a measurement resolution of $\lambda/12$. However, the linear interpolation has an error as the fringe shape at moderate level is not a saw-tooth strictly. In 2005 and 2006, Plantier, *et al.* [16] and Bes, *et al.* [17] presented a new displacement reconstruction algorithm suitable for moderate feedback level. In 2011, Fan, *et al.* [18] further improved the work in [16], [17] by fully considering the fringe shape at different feedback levels. This class of SMI-based displacement is suitable for a displacement larger than $\lambda/2$.

Another class of SMI-based displacement measurement method introduces a modulation to the SMI system through LD injection current or external cavity. This class can measure a displacement with high measurement resolution and the displacement can be less than $\lambda/2$. For example, in 1989, Suzuki, *et al.* reported to modulate the injection current with a sinusoidal waveform [19]. At each zero-crossing point of the modulation, the phase of the SMI signal can be detected. Thus, displacement measurements between two zero-crossing points can be obtained in a modulation period. The non-linearity of sinusoidal modulation may cause unexpected measurement error. In 1995, Kato, *et al.* used triangular/saw-tooth injection current into the SMI system [20]. The SMI system can generate a pulse train due to target displacement. The displacement is measured by detecting the phase shift for the pulse train between adjacent modulation periods with a resolution of 25 nm. In 1999, Suzuki, *et al.* also implemented displacement measurement with a triangular modulated injection current [21]. With phase-locked technique, the initial phase of the laser intensity signal correlated to the displacement can be obtained by measuring the feedback control current to the LD. The resolution is related to the modulation frequency of the feedback control system. In 2001, Ming Wang presented a system with a saw-tooth injection current [22]. By applying Fast Fourier transform (FFT) on an SMI signal at each modulation period, they can calculate the initial phase and thus the displacement. They claimed that the method can reached a precision of $\lambda/50$.

In the latter class of modulation-based displacement sensing systems reviewed above [20]–[22], displacement is obtained by detecting the initial phase of an SMI related signal at each modulation period. Thus, only one measurement point can be obtained within a modulation period. Hence, the measurement resolution is largely limited by the modulation frequency of the injection current. In addition, to acquire more accurate phase detection, the signal within a modulation period should contain many fringes. This will require a long initial distance between the LD and the target and high modulation magnitude. To relax these restrictions, in this paper, we propose a new method, where the phase of an SMI signal caused by displacement within each modulation period is considered to be time varying. A measurement formula is derived for calculating displacement by means of Fourier transform on the observed SMI signal [23], [24]. This time-frequency analysis method can measure the displacement for multiple points within a modulation period, hence improving the sensing performance.

The paper is organized as follows. In Section II, we introduce the basic principle of the FFT-based initial phase method for displacement measurement, and then the proposed algorithm is presented. In Section III, we present the details of simulations and experiments to test the performance of the proposed technique. Section IV concludes the paper.

II. A NEW ALGORITHM FOR SMI-BASED DISPLACEMENT SENSING

A. BACKGROUND THEORY

The SMI-based displacement measurement with modulated injection current is depicted in Fig. 1. The FFT-based algorithm for retrieving the initial phase of an SMI signal with weak feedback is summarized as below [22].

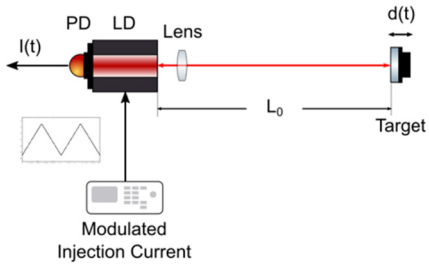

FIGURE 1. SMI-based displacement measurement with modulated injection current.

The laser intensity captured by the photodiode (PD) package at the rear of the LD is denoted as $I(t)$, expressed as:

$$I(t) = A(t) + B\cos\Phi(t), \tag{1}$$

where $A(t)$ is the linearly modulated output intensity without feedback, which corresponds to the injection current. In other words, when the waveform of injection current is given, $A(t)$ can be considered as known. Also, as $A(t)$ has nothing to do with the external optical feedback of the laser, it can be subtracted from (1) when the SMI signal is analyzed. B is the undulation coefficient. $\Phi(t)$ is the time varying light phase in the external cavity and $B\cos\Phi(t)$ is the conventional SMI signal for processing.

The phase $\Phi(t)$ is determined by both the laser frequency $\upsilon_0 + \gamma t$ and the external cavity length $L_0 + d(t)$, expressed as:

$$\begin{aligned}\Phi(t) &= 4\pi\frac{\upsilon_0+\gamma t}{c}(L_0+d(t)) \\ &= 4\pi\frac{\gamma t}{c}L_0+4\pi\frac{\upsilon_0}{c}L_0+4\pi\frac{\upsilon_0}{c}d(t)+4\pi\frac{\gamma t}{c}d(t),\end{aligned} \tag{2}$$

where υ_0 is the initial laser frequency, γ is the modulating efficient corresponding to optical frequency change, which can be regarded as a constant when the modulation frequency remains below tens of MHz [25], L_0 is the initial external cavity length, $d(t)$ is the displacement of target and c is the speed of light. To simplify (2), we introduce the carrier frequency $f_c = 2\gamma L_0/c$. We also denote the constant part of phase by $\phi_0 = 4\pi\upsilon_0 L_0/c$. $\phi(t) = 4\pi\upsilon_0 d(t)/c$ and it is the phase correlated to the displacement $d(t)$. The term $4\pi\gamma t d(t)/c$ can be neglected as it is very small compared to other terms in (2). Thus, (2) can be re-written as:

$$\Phi(t) \approx 2\pi f_c t + \phi_0 + \phi(t). \tag{3}$$

When the target moves very slowly, the displacement $d(t)$ can be considered as constant within each modulation period T of the injection current. We can obtain $\phi(t)$ by applying FFT on signal $B\cos\Phi(t)$ to get the phase of fringe signal, and thus the displacement $d(t)$. Obviously, the resolution associated with this method is limited by the modulation frequency of the injection current, as only a single measurement point can be obtained for $d(t)$ within each modulation period T. In other words, for measurement of a high-speed moving target, the injection current must be modulated by a high frequency signal, this is limited by the speed of LD's response. When the modulation frequency exceeds several tens of kilohertz, delay in the response of LD to current modulation will become significant, leading to the period of modulation unequal. Non-linearity in modulation waveform will also be remarkable and can cause large measurement error. To solve these problems, $d(t)$ should not be considered as a constant within each modulation period, and instead, it is time varying. We will develop a new algorithm for retrieving this time varying initial phase.

B. THE PROPOSED NEW ALGORITHM

As mentioned above, $A(t)$ in (1) is only dependent on the injection current, which can be considered as known and hence can be subtracted from (1). In the case of fixed target and modulated injection current, after subtracting $A(t)$, the laser intensity will be sinusoidal, which is called as the reference signal and denoted as:

$$I_0(t) = B_0\cos(2\pi f_c t + \phi_0). \tag{4}$$

Similarly, for the case of moving target with modulated injection current, the laser intensity after subtracting $A(t)$ is called as the SMI signal and can be expressed as:

$$I_1(t) = B_1\cos(2\pi f_c t + \phi_0 + \phi(t)), \tag{5}$$

where B_0, B_1 are the undulation coefficients determined by fixed and moving target respectively.

In order to obtain $\phi(t)$ from (4) and (5), we firstly sample the two signals at speed higher than the Nyquist rate (i.e., twice of the highest frequency component contained by the two signals), and within one modulation period, we have N samples, given by:

$$I_0(nT_s) = B_0\cos(\frac{2\pi f_c}{F_s}n + \phi_0), \tag{6}$$

and

$$I_1(nT_s) = B_1\cos(\frac{2\pi f_c}{F_s}n + \phi_0 + \phi(nT_s)), \tag{7}$$

where T_s and F_s are the sampling interval and frequency respectively. By applying Euler's expansion and FFT on (6), we have:

$$\begin{aligned}\widehat{I}_0(k) &= F(I_0(nT_s)) \\ &= F(\frac{B_0}{2}(e^{j(2\pi f_c T_s n+\phi_0)})) + F(\frac{B_0}{2}(e^{-j(2\pi f_c T_s n+\phi_0)})),\end{aligned} \tag{8}$$

where $F(\cdot)$ denotes the FFT operation. Equation (8) will yield N samples in the frequency domain. Due to the nature of the complex exponential, we can assume that there is no overlap between the contributions of the two terms on the right hand-side of (8) as the FFT results in the frequency domain. By setting an even number, the first half of the N FFT samples correspond to the first term of the right hand side of (8), and the second half of the N FFT samples correspond to the second term of the right hand side of (8). Therefore, by setting the following:

$$\widehat{I}_{0,a}(k) = \begin{cases}\widehat{I}_0(k) & for\ k = 1, 2, \ldots, N/2 \\ 0 & for\ k = N/2+1, \ldots, N\end{cases} \tag{9}$$

we have

$$\widehat{I}_{0,a}(k) = F(\frac{B_0}{2}(e^{j(2\pi f_c T_s n+\phi_0)})). \tag{10}$$

Hence by applying the inverse FFT on (10) we have

$$\frac{B_0}{2}(e^{j(2\pi f_c T_s n+\phi_0)}) = F^{-1}\left\{\widehat{I}_{0,a}(k)\right\}. \tag{11}$$

Similarly, we can apply FFT to (7), yielding:

$$\begin{aligned}\widehat{I}_{1,a}(k) &= F(I_1(nT_s)) \\ &= F(\frac{B_1}{2}(e^{j(2\pi f_c T_s n+\phi_0+\phi(nT_s))}) \\ &\quad + F(\frac{B_1}{2}(e^{-j(2\pi f_c T_s n+\phi_0+\phi(nT_s))})).\end{aligned} \tag{12}$$

Assuming that there is no overlap between the contribution of the two terms to the FFT results in the frequency domain, the first term on the right hand side of (12) will correspond to the first $N/2$ samples in the frequency domain, and the second half corresponds to the remaining $N/2$ frequency samples. Hence, we can set the following:

$$\widehat{I}_{1,a}(k) = \begin{cases}\widehat{I}_1(k) & for\ k = 1, 2, \ldots, N/2 \\ 0 & for\ k = N/2+1, \ldots, N\end{cases} \tag{13}$$

and

$$\widehat{I}_{1,a}(k) = F(\frac{B_1}{2}(e^{j(2\pi f_c T_s n+\phi_0+\phi(nT_s))})). \tag{14}$$

Note that (14) only holds if there is no overlap between $F(\frac{B_1}{2}(e^{j(2\pi f_c T_s n+\phi_0+\phi(nT_s))}))$ and $F(\frac{B_1}{2}(e^{-j(2\pi f_c T_s n+\phi_0+\phi(nT_s))}))$ in the frequency domain. Given $e^{j(2\pi f_c T_s n+\phi_0+\phi(nT_s))}$ a complex exponential signal with its phase modulated by $\phi(nT_s)$, its frequency spectrum will exhibits a band-pass surround the carrier frequency f_c, and the bandwidth depends on the rate of variance of $\phi(nT_s)$. Hence, when $\phi(t)$ varies significantly slower than the carrier frequency f_c, we can apply the inverse FFT on (14) to yield the following:

$$\frac{B_1}{2}(e^{j(2\pi f_c T_s n+\phi_0+\phi(nT_s))}) = F^{-1}\left\{\widehat{I}_{1,a}(k)\right\}. \tag{15}$$

Now we are able to detect the phase by considering the product of (15) and the complex conjugate of (11):

$$\frac{B_0 B_1}{4} e^{j\phi(nT_s)} = F^{-1}\left\{\widehat{I}_{1,a}(k)\right\}\left[F^{-1}\left\{\widehat{I}_{0,a}(k)\right\}\right]^*, \tag{16}$$

Therefore we have:

$$\phi(nT_s) = \arctan \frac{Im\left[F^{-1}\left\{\widehat{I}_{1,a}(k)\right\}\left[F^{-1}\left\{\widehat{I}_{0,a}(k)\right\}\right]^*\right]}{Re\left[F^{-1}\left\{\widehat{I}_{1,a}(k)\right\}\left[F^{-1}\left\{\widehat{I}_{0,a}(k)\right\}\right]^*\right]}. \tag{17}$$

Equation (17) is the formula to determine the phase correlated to the target displacement. As $\phi(t) = 4\pi\upsilon_0 d(t)/c$, we can retrieve the time varying displacement $d_r(t)$. It can be seen that for the number of samples we have for $I_1(t)$, the same number of phase points (thus displacement) can be obtained through (17). In addition, the undulation coefficients B_0 and B_1 do not affect the phase measurement in theory. Comparing to the existing techniques using initial phase detection, where only a single measurement point for displacement can be obtained, the proposed algorithm is able to obtain N points of displacement within each modulation period, and then is suitable for measurement of moving targets.

III. VERIFICATION OF THE PROPOSED METHOD

A. SIMULATION TEST

In order to test the performance of the proposed method, we conducted computer simulations on the case where injection current is modulated by a triangular waveform with a modulation period T_Δ. The modulation component $A(t)$ in (1) can be expressed as:

$$A(t) = \begin{cases} A_0 + 2A_\Delta t/T_\Delta, & t \in (nT_\Delta, \frac{2n+1}{2}T_\Delta) \\ A_0 + 2A_\Delta(1 - t/T_\Delta), & t \in (\frac{2n+1}{2}T_\Delta, (n+1)T_\Delta) \end{cases} \tag{18}$$

where A_0 is correlated to the DC offset and set as -50 mV in the simulation, A_Δ is the peak-peak value and n is an integer.

In the simulations we set $A_\Delta = 100$ mV, $T_\Delta = 0.01$ s (i.e., $F_\Delta = 100$ Hz), undulation coefficients $B_0 = 5$ mV, $B_1 = 6$ mV, carrier frequency $f_c = 1100$ Hz, initial external cavity length $L_0 = 15.5$ cm, laser wavelength $\lambda = c/\upsilon_0 = 830$ nm. In this case, term $4\pi\gamma td(t)/c$ in (2) is only 4.46^*10^{-4} rad and its influence can be neglected.

It should be pointed out that FFT should be carefully applied to each of the data blocks. Firstly, sample frequency must be integer multiple of the frequency of the injection current, i.e., F_s/F_Δ must be a positive integer. Spectral leakage will occur if this condition does not met. Secondly, the sample frequency must be higher than the Nyquist rate (i.e., twice of the highest frequency component). For the sake of simplicity, we only considered that number of samples is the power of 2, which is required by original FFT algorithm. When the number of samples is not the power of 2, we can pad zero-valued samples to make the total number of samples to be the power of 2 so that FFT can be applied. For the simulations, we choose 512-point FFT applying to half period of the modulation signal, and hence the sampling frequency should be $F_s = 102.4$ kHz. As the sampling frequency is about 100 times higher than the carrier frequency, the Nyquist condition should be met for both the reference signal and the SMI signal.

To verify the proposed algorithm, the main procedure of the simulation test is summarized as below:

1) Using (4) and (5) to generate the signals $I_0(t)$ and $I_1(t)$.
2) Obtaining 512 discrete samples by sampling $I_0(t)$ and $I_1(t)$ over a rising or falling part of $T_\Delta/2$, as shown by (6) and (7). Applying 512-point FFT on the two discrete sequences $I_0(nT_s)$ and $I_1(nT_s)$, as shown by (8) and (12).
3) Using (9) and (13) to obtain $\widehat{I}_{0,a}(k)$ and $\widehat{I}_{1,a}(k)$.
4) Using (17) to yield $\phi(nT_s)$ in each rising and falling part.
5) Repeating the step 2, 3 and 4 for all half modulation periods, and then we can calculate and retrieve the whole displacement.

Supposing a target is moving in sinusoidal vibration with $d(t) = d_0\cos(2\pi f_t t)$, where $d_0 = 100$ nm and $f_t = 10$ Hz. Fig. 2 shows the simulation results. The target displacement $d(t)$ and triangular modulation $A(t)$ are depicted in Fig. 2a,b. After removing the modulation $A(t)$, the reference signal $I_0(t)$ and SMI signal $I_1(t)$ each contains 11 fringes within each modulation period T_Δ, 5.5 fringes on each rising and falling part, as shown in Fig. 2c,d. Repeating the retrieving procedure for all half modulation periods, we can obtain the phase $\phi(t)$ and the retrieved displacement $d_r(t)$ comparing with $d(t)$ in a whole period of target displacement, as shown in Fig. 2e,f. The error between the two displacements is depicted in Fig. 2g. We evaluated the errors associated with the simulation results above. The maximum phase error in each rising and falling part is within 6.986^*10^{-4} rad, and the maximum displacement error in each part is within 0.0461 nm. Thus, the maximum relative error of the proposed method is $\max\frac{|d(t)-d_r(t)|}{\max|d(t),d_r(t)|}{}^*100\% = 0.0461\%$. In comparison, the method in [22] has a maximum phase

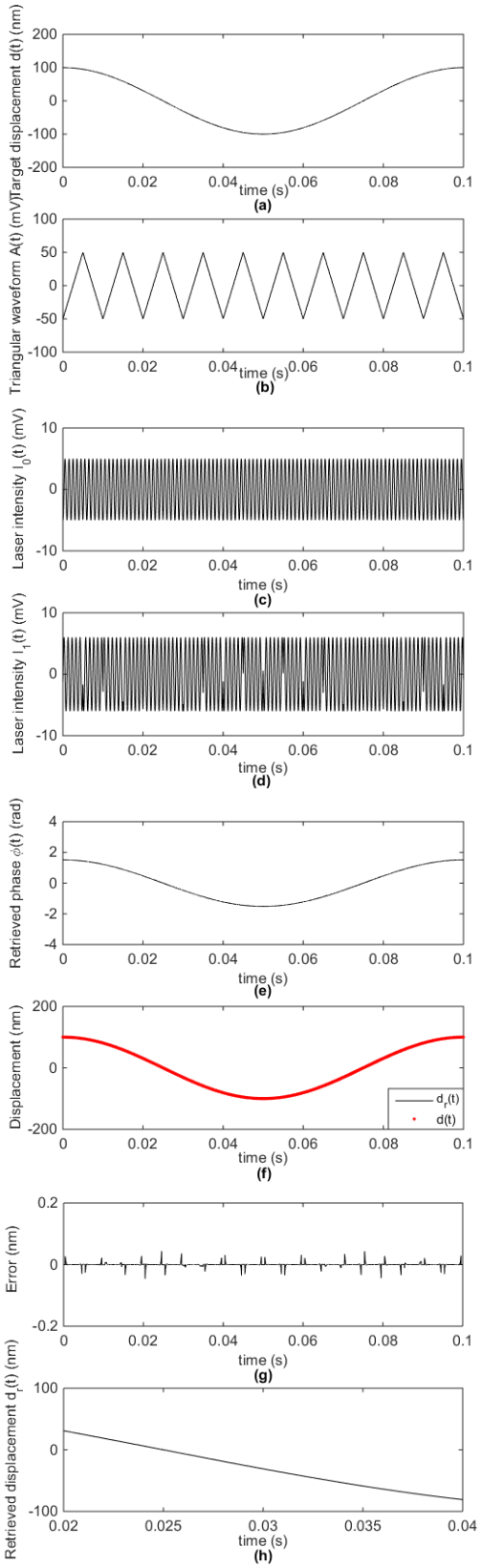

FIGURE 2. Simulation results for sinusoidal displacement. (a) The target displacement $d(t)$; (b) Triangular modulation $A(t)$; (c) Reference signal intensity $I_0(t)$ with fixed target; (d) SMI signal intensity $I_1(t)$ with moving target; (e) The obtained phase $\phi(t)$; (f) The comparison of the retrieved displacement $d_r(t)$ and $d(t)$; (g) The error between $d(t)$ and $d_r(t)$; (h) The detailed retrieved displacement between 0.02 s ∼ 0.04 s.

error of 0.2 rad and a maximum relative error of 1% for the displacement.

Another common problem associated with the application of FFT and inverse FFT on block based signals is the significant jumping error possibly occurring at the two edges of the signal block. In order to investigate such errors, we enlarged the results of the phase and displacement corresponding two periods of the injection current signal. As shown by Fig. 2h, no jumping error occurs between the two successive blocks, because all the parameters associated with the FFT are carefully chosen.

As the result shows, the retrieved target displacement matches well with the displacement set in the simulation. Within each rising and falling part of the triangle waves, the number of samples is $N = F_s^* T_\Delta/2 = 512$, which means 512 displacement points can be measured by the proposed algorithm, and the resolution is 512 times higher than existing methods in [20]–[22], where only one measurement point can be obtained.

As mentioned above the proposed method requires that the two terms on the right hand side of (12) do not overlap in frequency. For above example simulated, we have $d(t) = d_0 \cos(2\pi f_t t)$ and $f_t = 10$ Hz. As $\phi(t) = 4\pi \upsilon_0 d(t)/c$, the phase also varies sinusoidally at the frequency $f_t = 10$ Hz. As $f_t = 10$ Hz is significantly smaller than the carrier frequency $f_c = 1100$ Hz, the SMI signal still exhibits a very narrow band in frequency domain at f_c. As the sampling frequency F_s is much higher than f_c, it is reasonable to believe that overlap between the two terms on the right hand side of (12) can be ignored. In this case, we do not need to employ windowing techniques to reduce the influence of spectral spread of FFT components [26].

At the same time, based on our observation on the signals collected from experiments, there are fluctuations of below 3 mV in the amplitude of the signals (which is about 60mV). Thus we can assume that the signals contain a signal-to-noise ratio of higher than 25 dB. In order to test the influence of noise to the proposed algorithm, with the same parameters in Fig. 2, a Gaussian white noises of 25 dB is altered to both the $I_0(t)$ and $I_1(t)$, as shown in Fig. 3a,b. The retrieved displacement $d_r(t)$ is compared with $d(t)$ in Fig. 3c, and the error with noisy signals is depicted in Fig. 3d, with an amplitude of 4.97 nm and a relative error of 4.97%.

We also tested the proposed method for the cases of non-symmetric displacement. Supposing a target moves in a saw-tooth vibration with $d(t) = 2d_0 \times (f_t t - [f_t t]) - d_0$, where $d_0 = 100$ nm is the amplitude, $f_t = 100$ Hz is the vibration frequency and [] is the integer-valued function. Fig. 4 shows the simulation results. The target displacement $d(t)$ and triangular modulation $A(t)$ are depicted in Fig. 4a,b. After removing the modulation $A(t)$, the reference signal $I_0(t)$ and SMI signal $I_1(t)$ are shown in Fig. 4c,d, each containing 11 fringes within each period injection current modulation T_Δ. By applying the proposed method over all half modulation periods, we can obtain the phase $\phi(t)$ and the

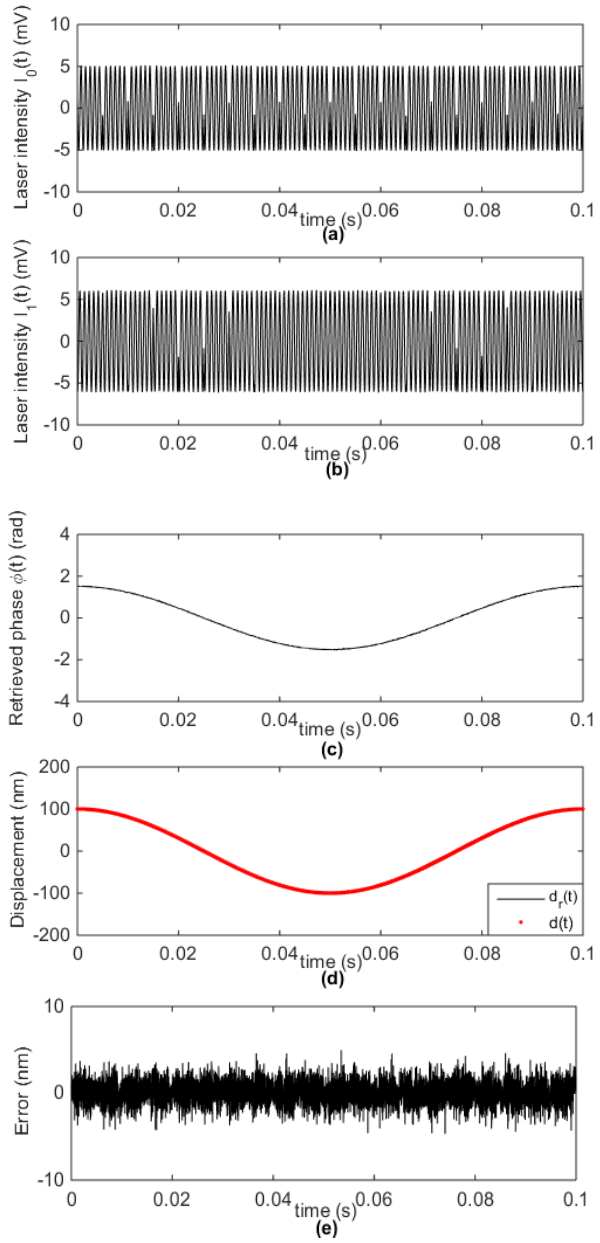

FIGURE 3. Simulation results for signals with noise. (a) Reference signal intensity $I_0(t)$ with fixed target; (b) SMI signal intensity $I_1(t)$ with moving target; (c) The obtained phase $\phi(t)$; (d) The comparison between retrieved displacement $d_r(t)$ and $d(t)$; (e) The error with noisy signals.

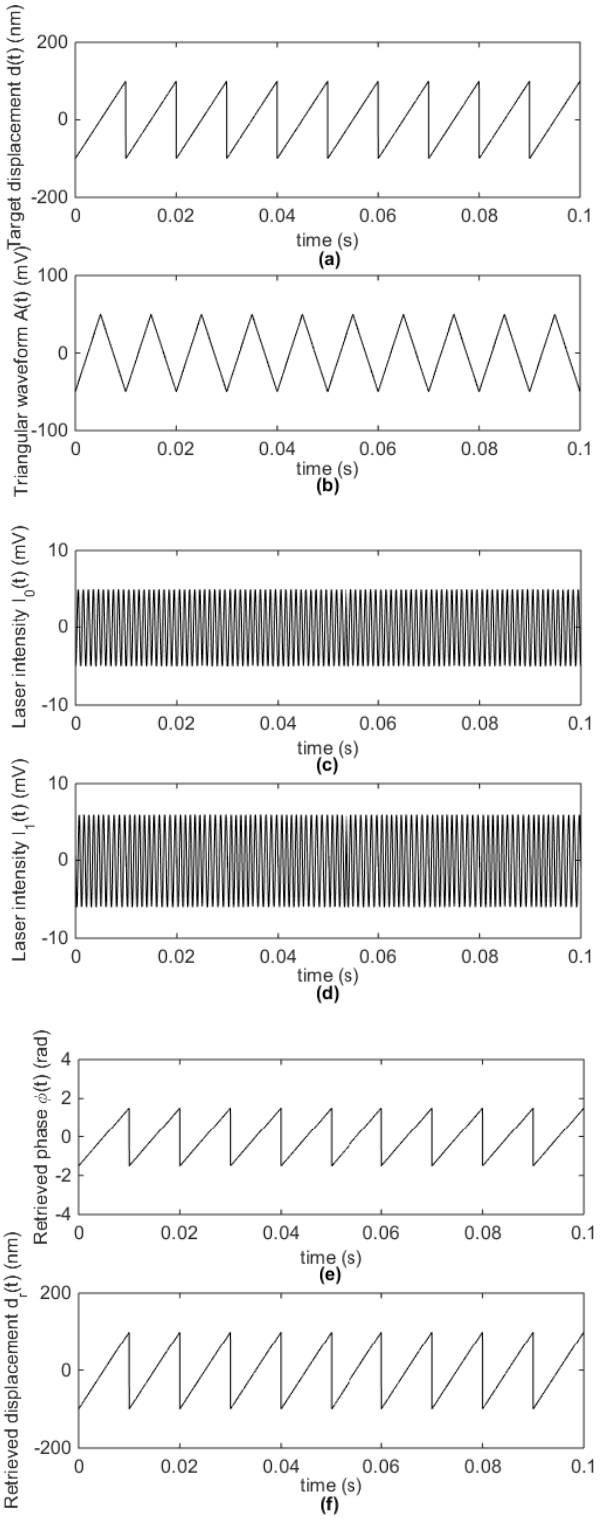

FIGURE 4. Simulation results for saw-tooth displacement. (a) The target displacement $d(t)$; (b) Triangular modulation $A(t)$; (c) Reference signal intensity $I_0(t)$ with fixed target; (d) SMI signal intensity $I_1(t)$ with moving target; (e) The obtained phase $\phi(t)$; (f) The retrieved displacement $d_r(t)$.

retrieved displacement $d_r(t)$ containing 10 periods of target displacement, as shown in Fig. 4e,f.

B. EXPERIMENTAL TEST

To further verify the proposed algorithm, an experimental system was built in our laboratory as depicted in Fig. 5. The LD in the experiment is a single mode LD (Hitachi HL8325G, $\lambda = 830$ nm, output power $P_0 = 40$ mW), which is driven and temperature-stabilized by an LD controller (Thorlabs, ITC4001). An injection current with triangular wave modulation is applied on the LD with DC offset of $65mA$, peak-peak value of 20 mA. The modulation period is $T_\Delta = 1$ ms. The temperature of the LD is stabilized at 23 ± 0.1°C. The laser emitted by the LD is focused by a lens and

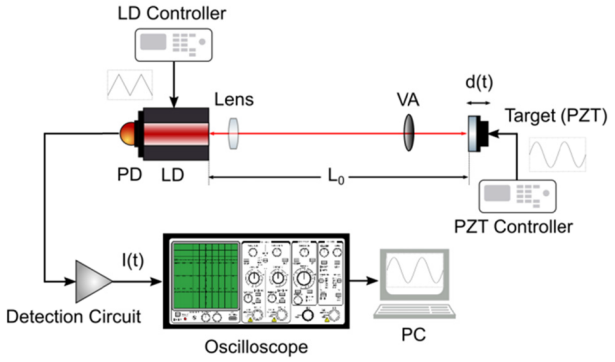

FIGURE 5. Experimental setup.

then hits a mirror as the external target. The mirror is glued on the surface of a piezoelectric actuator (Thorlabs, PZT, PAS005). The PZT is driven by a PZT controller (Thorlabs, MDT694) to provide a micro-displacement. A variable attenuator (VA) is inserted in between the lens and target to adjust the feedback level of the SMI system. The laser intensity of the modulated signals are detected by the PD packaged in the rear of the LD, further manipulated by a detection circuit, and finally captured and recorded by an oscilloscope (Tektronix, DSA 70804).

When applying sinusoidal vibration on the target, the maximum vibration frequency $f_{t\,\max}$ of the PZT is limited by the formula $f_{t\,\max} = \frac{I_{\max}}{\pi V_{pp} C}$, where $I_{\max}$ is the maximum driving current of the PZT driver, V_{pp} is the peak to peak driving voltage, and C is the capacitance of PZT. In the experiment, $I_{\max}$ of the PZT controller (MDT694) is 60 mA, V_{pp} is set as 500 mV to adjust an appropriate amplitude of micro-displacement, and C of the PZT (PAS005) is 20 μF. With this setup, the maximum vibration frequency $f_{t\,\max} = 1.91$kHz.

In the experiment, the initial external cavity length is $L_0 = 15.5$cm. The sinusoidal controlling voltage for the PZT is provided by a signal with $f_t = 100$ Hz and an amplitude of 250 mV, as shown in Fig. 6a, which results in a sinusoidal displacement with an amplitude of $d_0 = 67$ nm, as shown in Fig. 6b. While comparing to conventional methods, in order to treat the displacement as a constant within each modulation period, the vibration frequency of target is limited to 2 Hz in [22].

Before starting the experiment, we record the laser intensity without the PZT target, as shown in Fig. 6c. Then the PZT without its control signal is added to the system. The system is adjusted to work at a weak feedback regime. The laser intensity at this step is recorded as a reference signal. The reference signal after removing the modulation part is shown in Fig. 6d. Applying the driving signal to the PZT and recording the corresponding laser intensity signal, we obtained the SMI signal. The SMI signal after removing the triangular modulation part is shown in Fig. 6e. In the two figures, the signals collected contain an SNR about 25 dB. The carrier frequency f_c

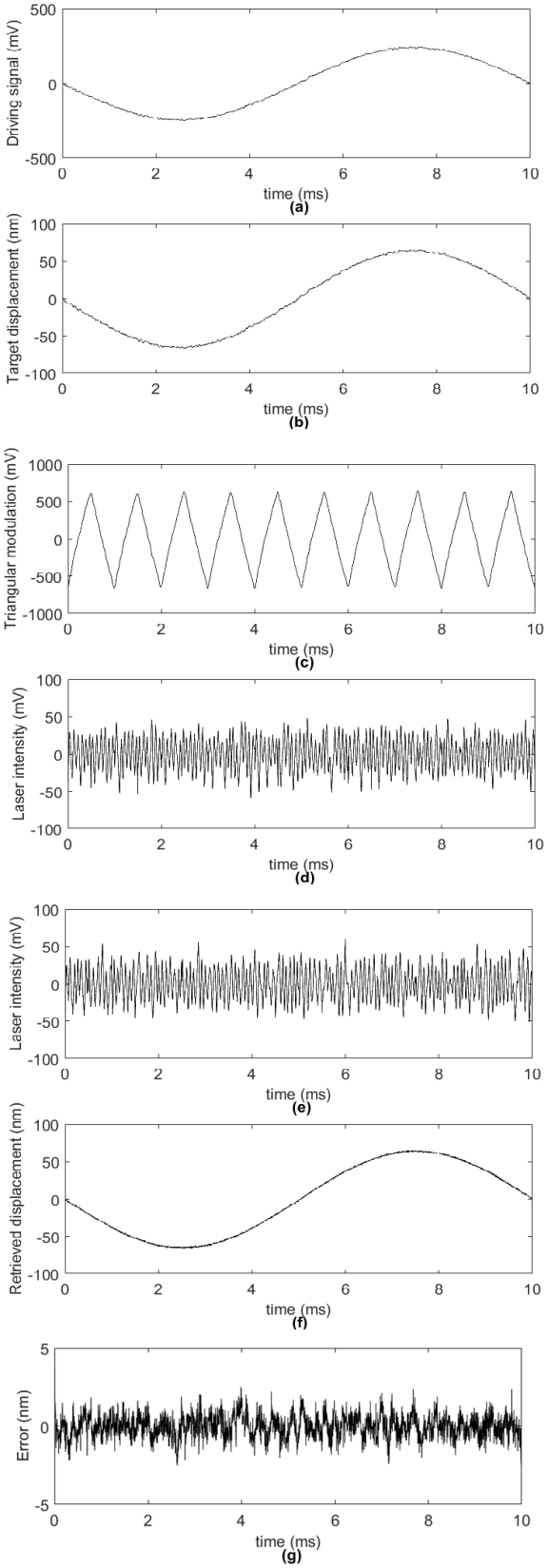

FIGURE 6. Experimental results. (a) The PZT driving signal corresponding to target displacement; (b) The target displacement; (c) Triangular modulation; (d) Reference signal intensity with fixed target; (e) SMI signal intensity with moving target; (f) The retrieved displacement; (g) The error between the original displacement and the retrieved displacement.

in the experiment is about 1300 Hz. We apply 512-point FFT on the signals and the sampling frequency $F_s = 1024$ kHz. Using the experimental data and following the measurement procedure described in simulation test, we are able to retrieve the displacement applied on PZT, as shown in Fig. 6f.

The error between the original displacement and the retrieved displacement is shown in Fig. 6g and the peak-peak amplitude of the error is 4.08 nm (or $\lambda/200$), while the experiment result in [22] contains an error of $\lambda/50$. The error might be resulted from multiple factors, e.g. the temperature change of LD, the non-linear reaction of PZT, the disorder of the amplifier circuit, etc. The experimental results again show that the proposed algorithm can retrieve the micro-displacement accurately. In this work, the main contribution is that we are able to obtain more measurement points for displacement within each modulation period. This will thus allow a target to move faster than the existing phase detection methods under same modulation condition.

IV. CONCLUSIONS

In this paper, we have proposed a new method to improve measurement performance for an SMI-based displacement sensing system. In the proposed method, the laser intensity of the SMI system with a fixed target is used as a reference signal. By applying FFT and IFFT to the SMI signal and the reference signal, we can obtain the phase of the SMI signal, thereby the displacement can be retrieved.

Based on the Nyquist sampling theorem, the highest frequency of a signal to be digitized should not exceed half of the sampling frequency. Hence the proposed technique is able to measure the displacement of target vibrating at the frequency up to half of the sampling frequency. The proposed method is able to yield N points of displacement results within each modulation period of injection current, where N is the number of samples of the SMI signal available. In contrast, the existing method can only produce a single measurement point on each period of injection current. Therefore, the proposed method is able to measure the displacement of a target vibrating at a frequency N times higher than the existing method, which is a significant performance increase.

REFERENCES

[1] J. Xi, Y. Yu, J. F. Chicharo, and T. Bosch, "Estimating the parameters of semiconductor lasers based on weak optical feedback self-mixing interferometry," *IEEE J. Quantum Electron.*, vol. 41, no. 8, pp. 1058–1064, Aug. 2005.

[2] S. Donati, "Developing self-mixing interferometry for instrumentation and measurements," *Laser Photon. Rev.*, vol. 6, no. 3, pp. 393–417, May 2012.

[3] O. D. Bernal, U. Zabit, and T. M. Bosch, "Robust method of stabilization of optical feedback regime by using adaptive optics for a self-mixing micro-interferometer laser displacement sensor," *IEEE J. Sel. Topics Quantum Electron.*, vol. 21, no. 4, pp. 336–343, Jul. 2015.

[4] M. Norgia, D. Melchionni, and A. Pesatori, "Self-mixing instrument for simultaneous distance and speed measurement," *Opt. Lasers Eng.*, vol. 99, pp. 31–38, Dec. 2017.

[5] C. Jiang, X. Wen, S. Yin, and Y. Liu, "Multiple self-mixing interference based on phase modulation and demodulation for vibration measurement," *Appl. Opt.*, vol. 56, no. 4, pp. 1006–1011, Feb. 2017.

[6] C. Yáñez, F. J. Azcona, and S. Royo, "Confocal flowmeter based on self-mixing interferometry for real-time velocity profiling of turbid liquids flowing in microcapillaries," *Opt. Express*, vol. 27, no. 17, pp. 24340–24352, Jul. 2019.

[7] Y. Ruan, B. Liu, Y. Yu, J. Xi, Q. Guo, and J. Tong, "Measuring linewidth enhancement factor by relaxation oscillation frequency in a laser with optical feedback," *Sensors*, vol. 18, no. 11, p. 4004, Nov. 2018.

[8] T. Taimre, M. Nikolić, K. Bertling, Y. L. Lim, T. Bosch, and A. D. Rakić, "Laser feedback interferometry: A tutorial on the self-mixing effect for coherent sensing," *Adv. Opt. Photon.*, vol. 7, no. 3, pp. 570–631, 2015.

[9] Y. Xiong, H. Chen, X. Wang, T. Feng, H. Yang, and W. Huang, "Improved method for damping coefficient measurement based on spectral analysis of a self-mixing signal," *Appl. Opt.*, vol. 59, no. 8, pp. 2386–2392, Mar. 2020.

[10] L. Shi, D. Guo, Y. Cui, H. Hao, W. Xia, Y. Wang, X. Ni, and M. Wang, "Design of a multiple self-mixing interferometer for a fiber ring laser," *Opt. Lett.*, vol. 43, no. 17, pp. 4124–4127, Sep. 2018.

[11] B. Liu, Y. Ruan, Y. Yu, J. Xi, Q. Guo, J. Tong, and G. Rajan, "Laser self-mixing fiber Bragg grating sensor for acoustic emission measurement," *Sensors*, vol. 18, no. 6, p. 1956, Jun. 2018.

[12] Y. Zhao, X. Shen, M. Zhang, J. Yu, J. Li, X. Wang, J. Perchoux, R. D. C. Moreira, and T. Chen, "Self-mixing interferometry-based micro flow cytometry system for label-free cells classification," *Appl. Sci.*, vol. 10, no. 2, p. 478, Jan. 2020.

[13] S. Donati, G. Giuliani, and S. Merlo, "Laser diode feedback interferometer for measurement of displacements without ambiguity," *IEEE J. Quantum Electron.*, vol. 31, no. 1, pp. 113–119, Jan. 1995.

[14] S. Merlo and S. Donati, "Reconstruction of displacement waveforms with a single-channel laser-diode feedback interferometer," *IEEE J. Quantum Electron.*, vol. 33, no. 4, pp. 527–531, Apr. 1997.

[15] N. Servagent, F. Gouaux, and T. Bosch, "Measurements of displacement using the self-mixing interference in a laser diode," *J. Opt.*, vol. 29, no. 3, p. 168, Jun. 1998.

[16] G. Plantier, C. Bes, T. Bosch, and F. Bony, "Auto adaptive signal processing of a laser diode self-mixing displacement sensor," in *Proc. IEEE Instrum. Meas. Technol. Conf.*, May 2005, pp. 1013–1017.

[17] C. Bes, G. Plantier, and T. Bosch, "Displacement measurements using a self-mixing laser diode under moderate feedback," *IEEE Trans. Instrum. Meas.*, vol. 55, no. 4, pp. 1101–1105, Aug. 2006.

[18] Y. Fan, Y. Yu, J. Xi, and J. F. Chicharo, "Improving the measurement performance for a self-mixing interferometry-based displacement sensing system," *Appl. Opt.*, vol. 50, no. 26, pp. 5064–5072, 2011.

[19] T. Suzuki, O. Sasaki, K. Higuchi, and T. Maruyama, "Real time displacement measurement in sinusoidal phase modulating interferometry," *Appl. Opt.*, vol. 28, no. 24, pp. 5270–5274, Dec. 1989.

[20] J. Kato, N. Kikuchi, I. Yamaguchi, and S. Ozono, "Optical feedback displacement sensor using a laser diode and its performance improvement," *Meas. Sci. Technol.*, vol. 6, no. 1, p. 45, Jan. 1995.

[21] T. Suzuki, S. Hirabayashi, O. Sasaki, and T. Maruyama, "Self-mixing type of phase-locked laser diode interferometer," *Opt. Eng.*, vol. 38, no. 3, pp. 543–548, Mar. 1999.

[22] M. Wang, "Fourier transform method for self-mixing interference signal analysis," *Opt. Laser Technol.*, vol. 33, no. 6, pp. 409–416, Sep. 2001.

[23] U. Zabit, O. D. Bernal, T. Bosch, U. Zabit, O. D. Bernal, and T. Bosch, "Time-frequency signal processing for a self-mixing laser sensor for vibration measurement," in *Proc. IEEE Sensors*, Oct. 2012, pp. 1–4.

[24] U. Zabit, O. D. Bernal, S. Amin, M. F. Qureshi, A. H. Khawaja, and T. Bosch, "Spectral processing of self-mixing interferometric signal phase for improved vibration sensing under weak-and moderate-feedback regime," *IEEE Sensors J.*, vol. 19, no. 23, pp. 11151–11158, Dec. 2019.

[25] T. Numai, "Advanced laser diodes and related devices," in *Laser Diodes and Their Applications to Communications and Information Processing*. Wiley, 2011, pp. 247–255.

[26] H. Wang, Y. Ruan, Y. Yu, J. Xi, Q. Guo, and J. Tong, "Effect of windowing on a sensing signal generated by self-mixing interferometry," *Proc. SPIE*, vol. 11197, Nov. 2019, Art. no. 111970F.

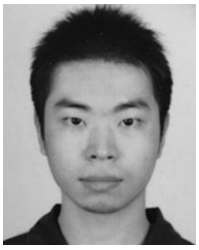

HAN WANG received the B.E. degree from the Beijing University of Posts and Telecommunications, China, in 2010, and the M.E. degree from Zhengzhou University, China, in 2015, respectively. He is currently pursuing the Ph.D. degree with the School of Electrical Computer and Telecommunications Engineering, University of Wollongong, Australia. His research interests include semiconductor lasers (SLs) with optical feedback, their applications on sensing and instrumentations, displacement measurement, and holography.

YUXI RUAN (Associate Member, IEEE) received the B.E. degree (Hons.) in telecommunication from the University of Wollongong, Australia, in 2015, where he is currently pursuing the Ph.D. degree with the Signal Processing for Instrumentation and Communications Research Laboratory. His research interests include optical feedback interferometry, optical sensing, and laser dynamics.

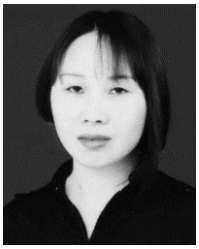

YANGUANG YU (Senior Member, IEEE) received the B.E. degree from the Huazhong University of Science and Technology, China, in 1986, and the Ph.D. degree from the Harbin Institute of Technology, China, in 2000.

She was with the College of Information Engineering, Zhengzhou University, China, on various appointments including a Lecturer, from 1986 to 1999, an Associate Professor, from 2000 to 2004, and a Professor, from 2005 to 2007. From 2001 to 2002, she was a Postdoctoral Fellow with the Opto-Electronics Information Science and Technology Laboratory, Tianjin University, China. She also had a number of visiting appointments including a Visiting Fellow at the Optoelectronics Group, Department of Electronics, University of Pavia, Italy, from 2002 to 2003, a Principal Visiting Fellow with the University of Wollongong, Australia, from 2004 to 2005, a Visiting Associate Professor and a Professor with the Engineering School, ENSEEIHT, Toulouse, France, in 2004 and 2006, respectively. She joined the University of Wollongong, in 2007, where she is currently an Associate Professor with the School of Electrical, Computer, and Telecommunications Engineering. Her research interests include semiconductor lasers with optical feedback and their applications in sensing and instrumentations, and secure chaotic communications. She is also interested in signal processing and its applications to 3-D profile measurement and telecommunication systems.

QINGHUA GUO (Senior Member, IEEE) received the B.E. degree in electronic engineering and the M.E. degree in signal and information processing from Xidian University, Xi'an, China, in 2001 and 2004, respectively, and the Ph.D. degree in electronic engineering from the City University of Hong Kong, Hong Kong, in 2008.

He is currently an Associate Professor with the School of Electrical, Computer, and Telecommunications Engineering, University of Wollongong, Wollongong, NSW, Australia, and an Adjunct Associate Professor with the School of Engineering, University of Western Australia, Perth, WA, Australia. His current research interests include signal processing and telecommunications.

Dr. Guo was a recipient of the Australian Research Council's Discovery Early Career Researcher Award.

JIANGTAO XI (Senior Member, IEEE) received the B.E. degree in electrical engineering from the Beijing Institute of Technology, Beijing, China, in 1982, the M.E. degree in electrical engineering from Tsinghua University, Beijing, China, in 1985, and the Ph.D. degree in electrical engineering from the University of Wollongong, Wollongong, NSW, Australia, in 1996.

He was a Postdoctoral Fellow with the Communications Research Laboratory, McMaster University, Hamilton, ON, Canada, from 1995 to 1996, and a Technical Staff Member with Bell Laboratories, Lucent Technologies Inc., Murray Hill, NJ, USA, from 1996 to 1998. He was the Chief Technical Officer with TCL IT Group Company, Huizhou, China, from 2000 to 2002. In 2003, he rejoined the University of Wollongong, as a Senior Lecturer, and he is currently a Full Professor and the Head of School of Electrical, Computer, and Telecommunications Engineering. His current research interest includes signal processing and its applications in various areas, such as instrumentation and measurement, as well as communications.

JUN TONG (Member, IEEE) received the B.E. and M.E. degrees from the University of Electronic Science and Technology of China (UESTC) and the Ph.D. degree in electronic engineering from the City University of Hong Kong. He is currently a Senior Lecturer with the School of Electrical, Computer, and Telecommunications Engineering, University of Wollongong, Australia. His research interest includes signal processing and its applications to communication systems.